**Supporting Information**

# Revealing the True Impact of Interstitial and Substitutional Nitrogen Doping in $TiO_2$ on Photoelectrochemical Applications

Sherdil Khan[a*] Thais L. Ruwer[b], Niqab Khan[a], Ariadne Köche[c], Rhys W. Lodge[d], Horácio C. Júnior[e], Rubem L. Sommer[e], Marcos J. L. Santos[c], Célia F. Malfatti[b], Carlos P. Bergmann[b] and Jesum Alves Fernandes[d*]

[a.] *Programa de Pós-Graduação em Física (PPGFIS) and Programa de Pós-Graduação em Materiais (PPGCIMAT), Federal University of Rio Grande do Sul (UFRGS), Campus do Vale: Av. Bento Gonçalves, 9500 - Agronomia, Porto Alegre - RS, Brazil.*

[b.] *Programa de Pós-Graduação em Engenharia de Minas, Metalúrgica e de Materiais (PPGE3M), Universidade Federal do Rio Grande do Sul, Av. Bento Gonçalves, 9500, 91501-970 Porto Alegre, RS, Brazil.*

[c.] *Programa de Pós-Graduação em Química (PPGQ) and Programa de Pós-Graduação em Materiais (PPGCIMAT), Federal University of Rio Grande do Sul (UFRGS), Campus do Vale: Av. Bento Gonçalves, 9500 - Agronomia, Porto Alegre - RS, Brazil.*

[d.] *School of Chemistry, University Park, Nottingham NG7 2RD, University of Nottingham, UK.*

[e.] *Centro Brasileiro de Pesquisas Físicas (CBPF), Rua Dr. Xavier Sigaud 150, Urca - Rio de Janeiro-RJ, Brazil.*

*sherdil.khan@ufrgs.br, Jesum.Alvesfernandes@nottingham.ac.uk*

Electron microscopy of $TiO_2$ NTs

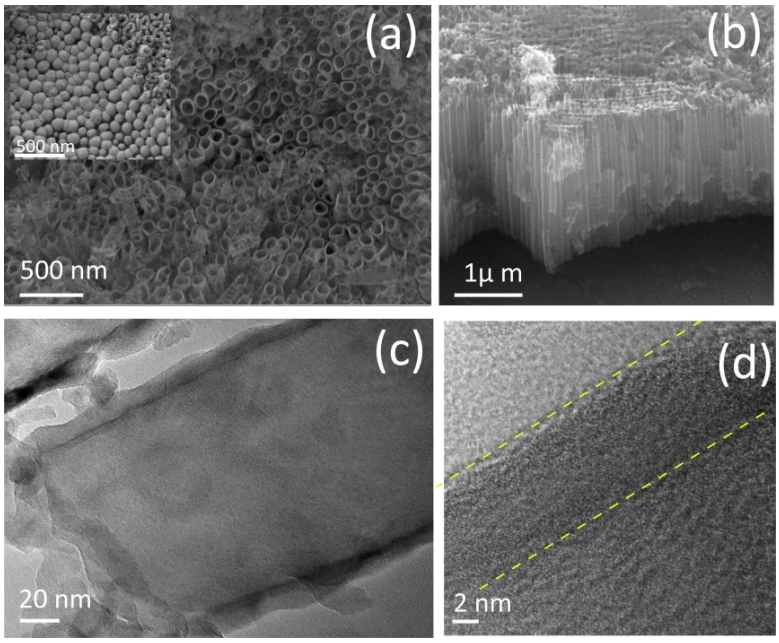


**Figure S1.** FEG-SEM images taken from the scratched area of as-anodized amorphous $TiO_2$ nanotubes, (a) top view (in set: bottom view) and (b) cross section view. TEM images of the same sample taken after thermal treatment of 400 °C in air for 3h (named as pure $TiO_2$), (c) cross section view and (d) high magnification view of the tube walls, encompassed by the two dashed yellow lines.

The as-anodized nanotubes had open tops and closed bottoms with smooth walls and the heat treatment at 400°C in air did not affect the tubular morphology (Figure S1). In FEG-SEM images, the top of the pure $TiO_2$ nanotubes (Figure S2a) did not differ much when compared to the as-anodized nanotubes (Figure S1a), TN-400 (Figure S2b) and TN-500 (Figure S1c). On the other hand, the top of TN-600 (Figure S2d) presented small cracks which were intense for TN-700 (Figure S2e) along with the agglomeration of the nanotubes at some spots marked in the figure. TN-800 top (Figure S2f) was totally collapsed showing that the nanotubes could withstand nitridation temperatures up to 700 °C. However, in the tape scratching test, TN-700 easily exfoliated from the substrate compared to lower temperature nitrided samples. This may be related to their weak adherence arising from the interfacial stress between the nitrided substrate and the nanotubes having different crystal structure. The cross-section views (Figure S2g – 2i) show that the nanotubes are vertically oriented with preserved tubular morphology.

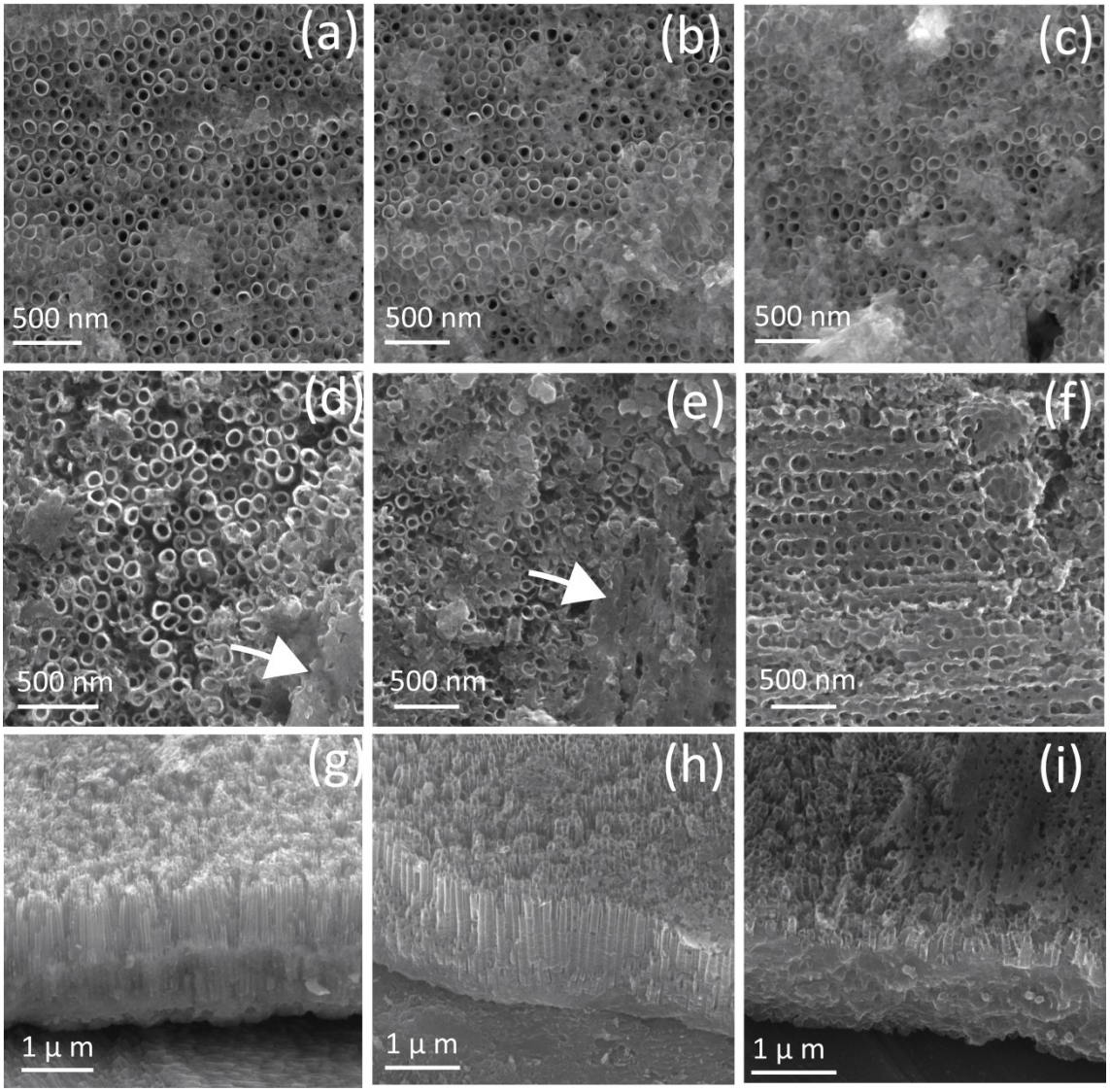


**Figure S2.** Top view FEG-SEM images of (a) pure $TiO_2$ nanotubes (b) TN-400, (c) TN-500, (d) TN-600, (e) TN-700 and (f) TN-800. Cross sections of (g) TN-500, (h) TN-600 and (i) TN-700.

## PXRD of $TiO_2$ NT and nitride samples

The sharp diffraction peaks at 35.1º, 38.4° and 53.4° correspond to the Ti substrate (marked as α). The XRD patterns identified all of the phases present in $TiO_2$ nanotubes. The intense peaks from the Ti substrate masked smaller peaks that were not visible in the diffractograms; therefore, to decrease the substrate contribution, grazing angle XRD patterns were recorded at a very small grazing angle of 0.5° (Figure 3). In addition, ramp rate for a fixed nitridation temperature (400 °C) did not affect the crystal structure so we focused the analysis on the 10 °C/min samples (Table S1).

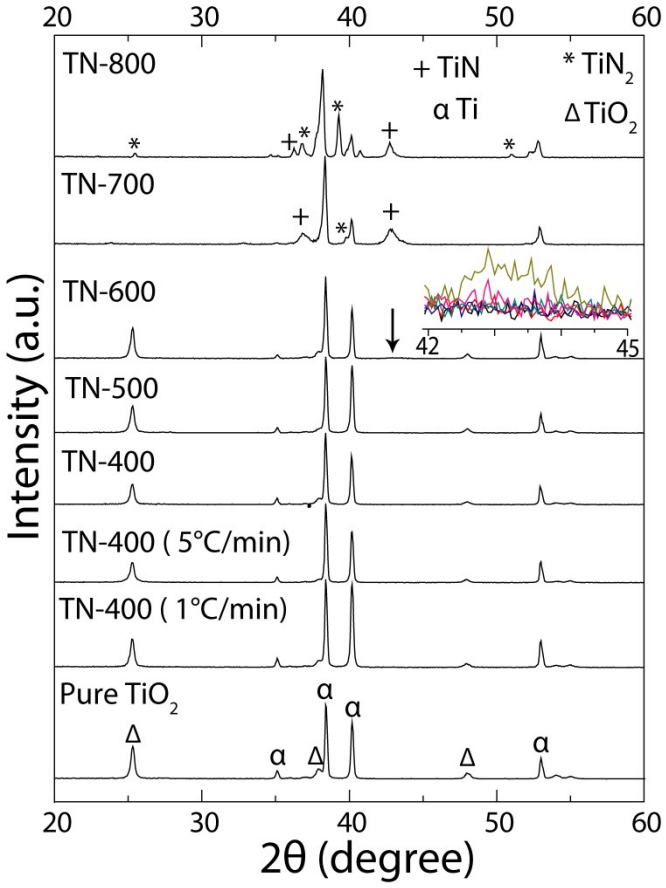


**Figure S3.** XRD patterns of $TiO_2$ nanotubes as a function of nitridation temperature and heat ramping.

**Table S1.** Crystallite grain size, calculated using the Scherrer equation, and $I_{(101)}/ I_{(200)}$ ratios taken from PXRD. Ramp rates were 10 °C/min to the respective temperatures unless stated otherwise.

| Name | Grain size (nm) | Ratio of intensities from anatase |
|---|---|---|

| | | (101) and (200) peaks ($I_{(101)}$/ $I_{(200)}$) |
|---|---|---|
| Pure $TiO_2$ | 24.1 | 5.7 |
| TN-400 (1 °C/min) | 22.1 | 7.2 |
| TN-400 (5 °C/min) | 21.6 | 6.3 |
| TN-400 | 21.9 | 7.4 |
| TN-500 | 21.4 | 6.4 |
| TN-600 | 21.2 | 6.7 |
| TN-700 | N/A | N/A |
| TN-800 | N/A | N/A |

## XPS Binding Energies

**Table S2.** Binding energy values obtained from the peaks fitting of the XPS spectra

| Entry | B.E of Ti 2p | | | | | |
|---|---|---|---|---|---|---|
| | Peak 1 | | Peak 2 | | Peak 3 | |
| | Ti $2p_{3/2}$ | Ti $2p_{1/2}$ | Ti $2p_{3/2}$ | Ti $2p_{1/2}$ | Ti $2p_{3/2}$ | Ti $2p_{1/2}$ |
| TN-400 | 458.9 | 464.6 | - | - | - | - |
| TN-500 | 458.8 | 464.5 | - | - | - | - |
| TN-600 | 458.5 | 464.2 | 456.5 | 462.5 | - | - |
| TN-700 | 458.5 | 464.2 | 456.8 | 462.8 | 455.6 | 461.6 |
| TN-800 | 458.6 | 464.3 | 456.6 | 462.6 | 455.5 | 461.5 |

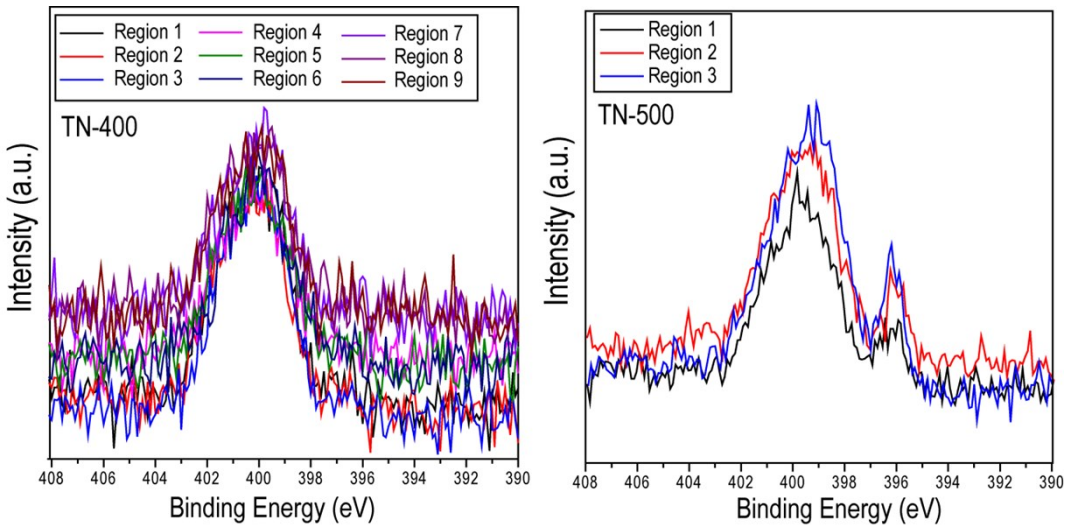


**Figure S4.** High resolution XPS spectra of N1s region of TN-400 and TN-500 acquired from the multiple areas of the same sample.

It can be seen that TN-400 exhibited only one peak in the N1s region at ~400 eV, related to interstitial N-doping. On the other hand, TN-500 exhibited two peaks; one at ~400 eV and another at ~396 eV, related to substitutional doping. These results demonstrated that the data was reproducible as the interstitial doping dominates at temperatures up to 400°C and the substitutional doping occurs at higher temperatures.

## Elemental mapping

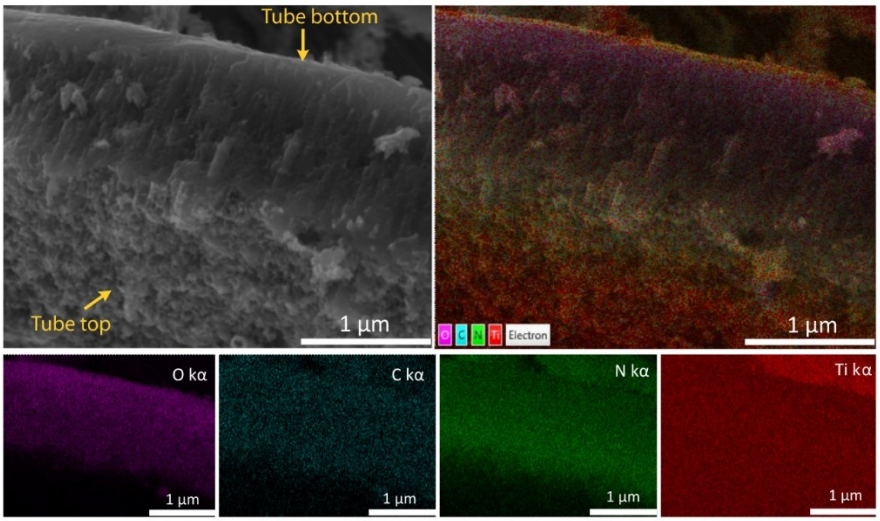


**Figure S5.** EDS elemental mapping of TN-700 showing the distribution of O, C, N and Ti in the samples. The top and the bottom of the NTs are marked with the arrows in the image. Comparing Ti, O and N gradients it can be seen the top of the tubes contains large Ti content as compared to other elements.

## UV-vis diffuse reflectance

Figure S5 displays UV-diffused reflectance of nitrided samples. The samples have progressively changed their color with nitridation temperature. Visually, TN-400 and TN-500 were not different in color compared to pure $TiO_2$; however, TN-600 appeared slightly bluish. In the literature, the color change is related to the formation of lower oxidation state species (e.g. $Ti^{3+}$) in the crystal lattice that act as color centers; thereby, electron donor states are created below the CB.[1] Depending on the photocatalytic reaction, such states may act as recombination centers for photogenerated charge carriers or they can act as current flow sites to enhance charge transfer efficiency.[2–4]

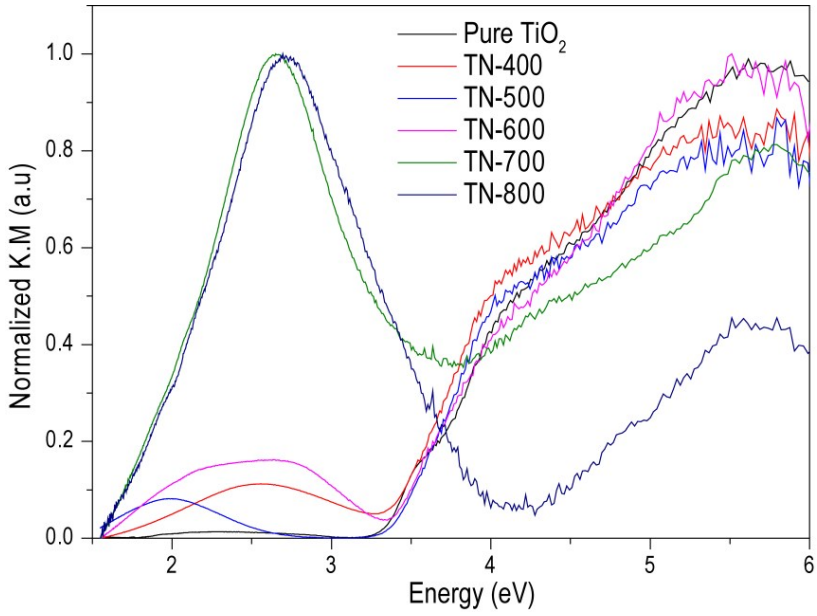


| Sample | Bandgap (eV) |
|---|---|
| Pure $TiO_2$ | 3.31±0.02 |
| TN-400 | 3.28±0.04 |
| TN-500 | 3.30±0.02 |
| TN-600 | 3.27±0.05 |
| TN-700 | N/A |
| TN-800 | N/A |

**Figure S6.** UV-Vis diffuse reflectance of N doped $TiO_2$ prepared under different nitridation temperatures for a fixed gas flux of 100 mL/min. These were used to estimate the bandgap values that are shown in the adjacent table.

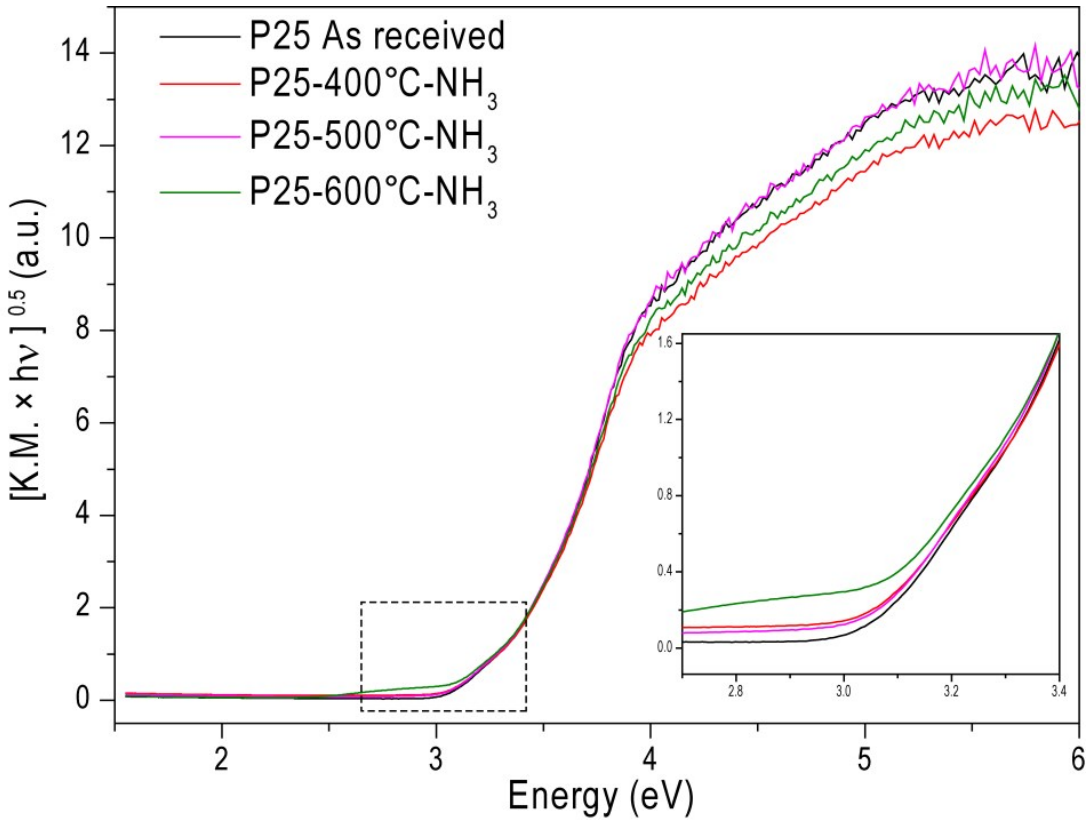


**Figure S7.** UV-Vis diffuse reflectance of P25 nitrided at different temperatures for a fixed gas flux of 100 mL/min for 3 h. The inset shows the amplified absorption spectra of the region marked as dotted rectangle emphasizing on the transitions above the bandgap.

## Photocurrent at varying flux rate, stability and IPCE of the photoelectrodes

TN-400 gave the best photocurrent compared to TN-500 and TN-600 and, therefore, it was chosen as the candidate to study the flux variation effect on PEC performance (Figure S8) and stability test under water oxidation (Figure S9). The photocurrent responses were still low and do not differ much from each other (Figure S8) suggesting that gas flux rate does not influence the electronic structure of the N doped $TiO_2$ and hence the photocurrent.

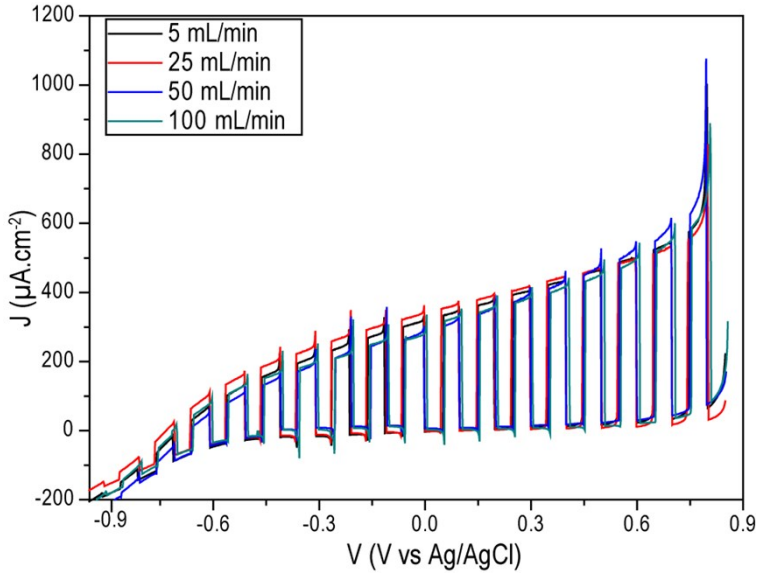


**Figure S8.** LSV curves from the samples prepared at variable flux rate and a fixed temperature of 400 °C collected in $Na_2S$ (0.24 M) and $Na_2SO_3$ (0.35 M).

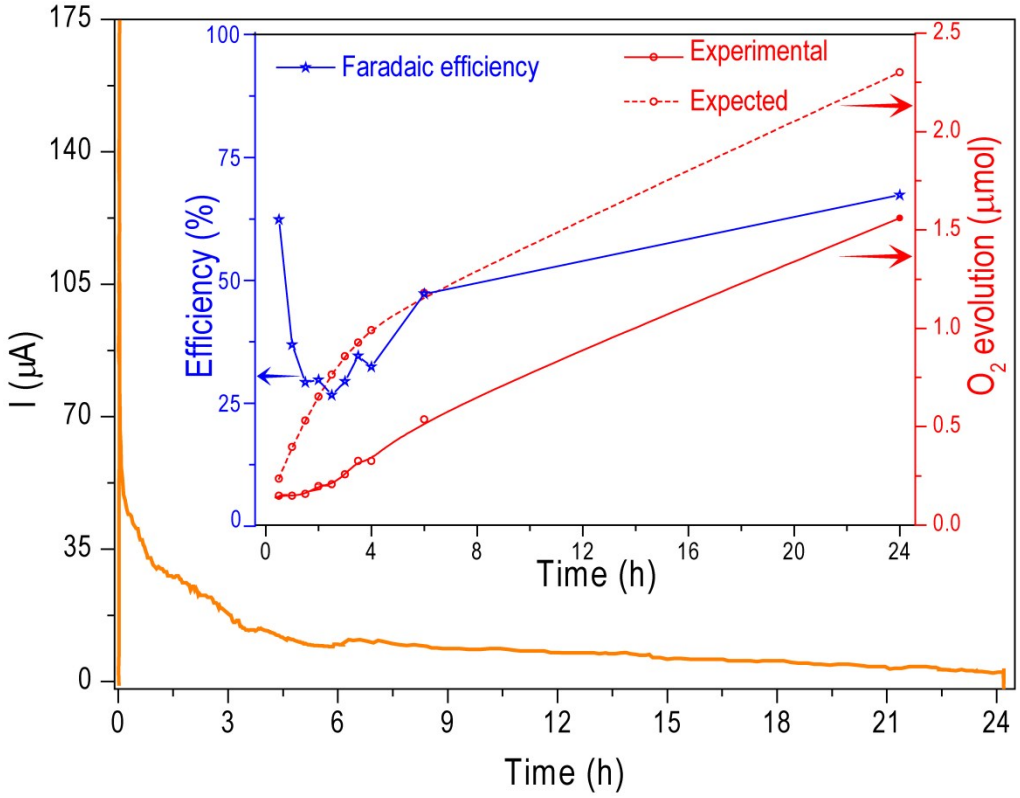


**Figure S9. (a)** Chronoamperometric (I-t) curves for TN-400 collected in KOH (1M) at 0 V in two electrodes configuration. The inset shows the experimental and expected $O_2$ evolutions based on the photocurrent and the respective Faradaic efficiencies. The lines are drawn to guide the eye. The photocurrent was drastically decayed within first few minutes of the experiment.

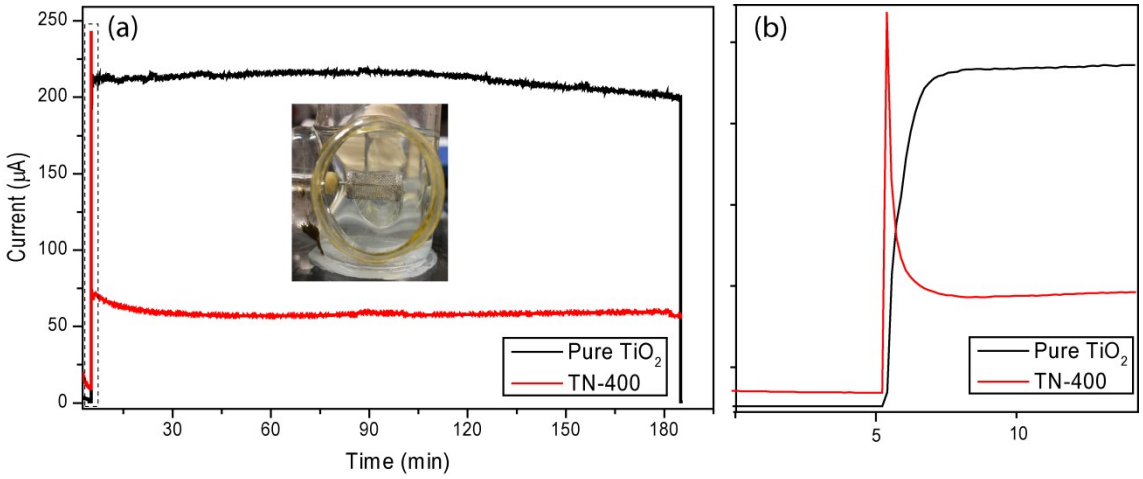


**Figure S10. (a)** Chronoamperometric (I-t) curves of Pure $TiO_2$ and TN-400 collected in $Na_2S$ (0.24 M) and $Na_2SO_3$ (0.35 M) at 0 V in two electrodes configuration. The inset shows the Pt electrode with $H_2$ gas bubbles trapped in the mesh. **(b)** I-t curve amplified at the beginning of the process, highlighting anodic overshoot observed for TN-400.

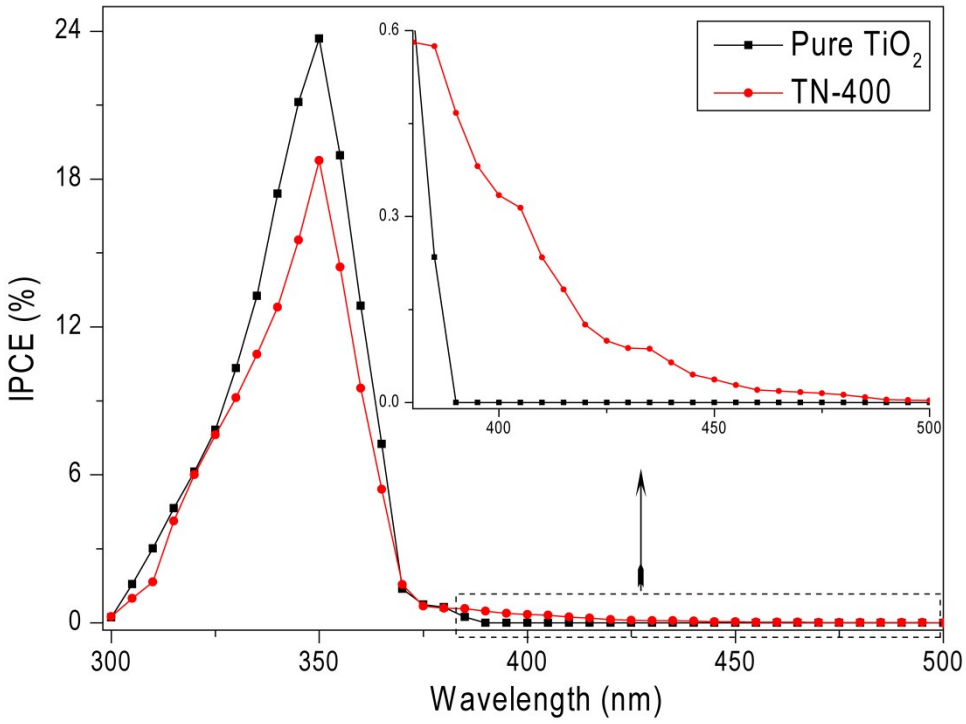


**Figure S10.** IPCE spectra of pure $TiO_2$ and TN-400 collected in $Na_2S$ (0.24 M) and $Na_2SO_3$ (0.35 M). The inset shows the amplified IPCE spectra of the region marked as dotted rectangle emphasizing on the visible light absorption characteristics of TN-400 due to N-doping.

## References


1 Y. C. Nah, I. Paramasivam and P. Schmuki, *ChemPhysChem*, 2010, **11**, 2698–2713.

2 B. Klahr, S. Gimenez, F. Fabregat-Santiago, J. Bisquert and T. W. Hamann, *Energy Environ. Sci.*, 2012, **5**, 7626–7636.

3 M. Nishida, *J. Appl. Phys.*, 1980, **51**, 1669–1675.

4 H. Li, S. Wu, Z. D. Hood, J. Sun, B. Hu, C. Liang, S. Yang, Y. Xu and B. Jiang, *Appl. Surf. Sci.*, 2020, **513**, 145723.